HHS Public Access

Author manuscript

Nat Chem. Author manuscript; available in PMC 2021 December 01.

Published in final edited form as:

Nat Chem. 2021 June ; 13(6): 540–548. doi:10.1038/s41557-021-00660-y.

Stereo- and regiodefined DNA-encoded chemical libraries enable efficient tumour-targeting applications

Nicholas Favalli[1], **Gabriele Bassi**[1], **Christian Pellegrino**[1], **Jacopo Millul**[2], **Roberto De Luca**[2], **Samuele Cazzamalli**[2], **Su Yang**[3], **Anika Trenner**[4], **Nour L. Mozaffari**[4], **Renier Myburgh**[5], **Mustafa Moroglu**[6], **Stuart J. Conway**[6], **Alessandro A. Sartori**[4], **Markus G. Manz**[5], **Richard A. Lerner**[7], **Peter K. Vogt**[3], **Jörg Scheuermann**[*,1], **Dario Neri**[*,1]

[1]Department of Chemistry and Applied Biosciences, Swiss Federal Institute of Technology (ETH Zürich), Zürich, Switzerland.

[2]Philochem AG, Otelfingen, Switzerland.

[3]Scripps Research Institute, Department of Molecular Medicine, La Jolla, California 92037, USA.

[4]Institute of Molecular Cancer Research, University of Zürich, Zürich, Switzerland.

[5]Department of Medical Oncology and Hematology, University Hospital Zurich and University of Zurich, Comprehensive Cancer Center Zurich (CCCZ), 8091 Zurich, Switzerland.

[6]Department of Chemistry, Chemistry Research Laboratory, University of Oxford, Mansfield Road, Oxford, OX1 3TA, UK.

[7]Scripps Research Institute, Department of Chemistry, La Jolla, California 92037, USA.

Abstract

The encoding of chemical compounds with amplifiable DNA tags facilitates the discovery of small molecule ligands for proteins. In order to investigate the impact of stereo- and regio-chemistry on ligand discovery, we synthesized a DNA-encoded library of 670,752 derivatives based on 2-azido-3-iodophenylpropionic acids. The library was selected against multiple proteins and yielded specific ligands. The selection fingerprints obtained for a set of protein targets of pharmaceutical

[*] Corresponding authors: D.N.: phone: +41-44-6337401, dario.neri@pharma.ethz.ch, J.S.: phone: +41-44-6337774, joerg.scheuermann@pharma.ethz.ch.

Author contributions

N.F., J.S., D.N. designed the project. N.F. constructed the library. N.F. and G.B. performed affinity selections and analyzed the HT-Sequencing results. J.S. helped with the evaluation of HT-Sequencing. C.P. performed the FACS and uniCAR-T killing assay experiments. J.M. and S.C. performed ex-vivo experiments on SK-RC-52 positive mice. R.D.L. produced hTNC and mTNC. S.Y. and P.K.V. constructed the expression vectors for the PI3K proteins and carried out the large-scale production in insect cells and the purification of these proteins. A.T, N.M. and A.A.S. produced CtIP proteins. R.M. and M.G.M. were involved in the cloning of the UniCAR plasmid. M.M. and S.J.C. produced CREBBP and BRD4(1) proteins. N.F. performed the resynthesis and the validation of all hit compounds. The manuscript was written through contributions of all authors. The manuscript was written by N.F., R.A.L., J.S., D.N. and corrected by all authors.

Competing Interests Statement

D.N. is co-founder and shareholder of Philochem AG (http://www.philochem.com), a company active in the field of DNA-encoded chemical libraries.

Data availability.

The main data supporting the findings of this study are available within this Article and its Supplementary Information. Extra data and materials are available from the corresponding authors upon reasonable request. Software for the evaluation of high-throughput DNA sequencing has been previously reported[87].

relevance clearly showed the preferential enrichment of *ortho*-, *meta*- or *para*-regioisomers, which was experimentally verified by affinity measurements in the absence of DNA. The discovered ligands included novel selective enzyme inhibitors and binders to tumor-associated antigens, enabling conditional chimeric antigen receptor T (CAR-T) cell activation and tumor targeting.

Graphical abstract

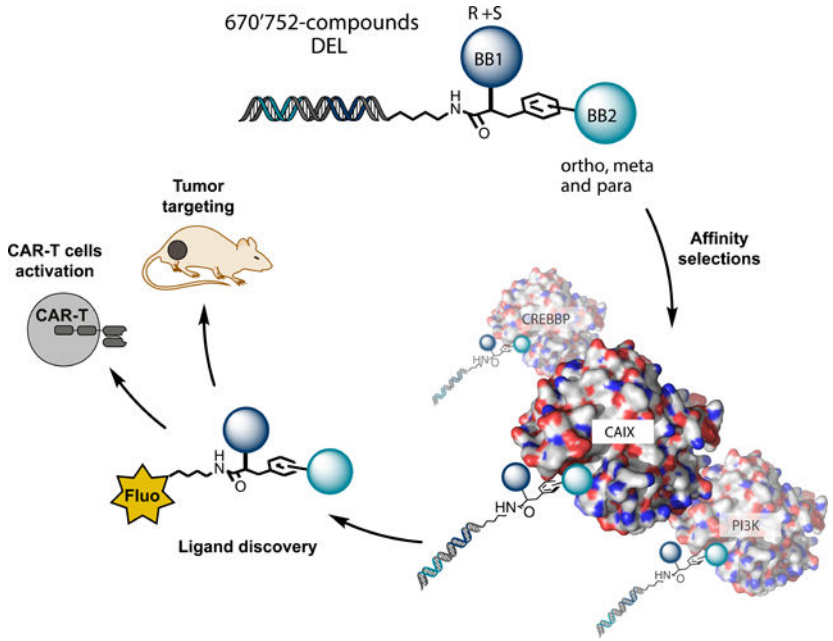

Keywords

DNA-encoded chemical libraries; stereochemistry; regiochemistry; Suzuki coupling; Sonogashira coupling; Chimeric Antigen Receptor T cells (CAR-T)

There is a growing interest in the use of DNA-encoded chemical libraries (DELs) as tools for the discovery of small organic ligands against target proteins. The identification of such compounds plays an important role in Pharmaceutical research and in Chemical Biology[1–9]. The concept of encoding molecules with DNA barcodes, first postulated in 1992[10], has now found widespread applications for the discovery of ligands against targets of biochemical or pharmacological interest. By employing split-and-pool synthetic methodologies[11–13], DNA-templated synthesis strategies[14] or DNA self-assembling procedures[15,16], libraries with large combinatorial diversity can be created, starting from a moderately-sized set of oligonucleotides and building blocks.

In full analogy to antibody phage-display libraries[17,18], DELs can be screened by affinity panning on proteins immobilized on solid supports. The high-throughput sequencing of the DNA barcodes before and after selection allows the facile identification of preferentially enriched ligands, which can be subsequently resynthesized for confirmation of binding affinity[3,4,6–9]. While antibody phage display libraries typically yield binders against virtually all purified protein antigens used as bait[19], only a few systematic studies have

documented the success rate of DELs for hit discovery, so far[20,21]. In order to increase the probability of isolating binders from DELs, one may consider to expand library size[22]. This may lead to an unacceptable growth of molecular weight if three or more sets of building blocks are used, or may require substantial investments for the purchase of a large number of building blocks. Chemical strategies aimed at creating structural diversity starting from relatively compact scaffolds may help explore chemical space and facilitate hit identification, while avoiding the creation of molecules that would violate Lipinski's rule of five[23–25].

Our group[23], and the group of Stuart Schreiber[26], have described initial library construction activities for the incorporation of stereochemical diversity and topographic complexity into DELs, as an avenue to explore a larger chemical space and discover selective binders against proteins of biomedical interest[27,28]. DELs are increasingly being considered as tools for ligand discovery, but library size alone does not guarantee success in screening campaigns[13,27,29]. Both chemical purity (which directly depends on the robustness of the employed reactions for library synthesis) and library design contribute to the productive discovery of binders against "hard-to-drug" targets[3,4,6].

Recent reports have shown how the discovery of small ligands, which selectively localize at the site of disease, may open novel biomedical applications. Small molecule-drug conjugates (SMDCs) are increasingly being considered as an alternative to antibody-drug conjugates (ADCs) for superior pharmacodelivery applications[30,31]. Fluorescein-labeled chemical adaptors have been used as "bridge" molecules between tumor cells and engineered T cells carrying an anti-fluorescein antibody on their surface ("Universal CAR-T cells"), thus allowing the selective killing of neoplastic cells [32–35]. Small molecule adaptors diffuse into tissue more efficiently than antibodies and clear more rapidly from circulation, helping spare normal tissues[30].

In this article, we functionalized 2-azido-3-iodophenylpropionic acid derivatives in order to construct a DEL with structural diversity both in terms of amino acid stereochemistry and of regiochemistry of phenyl ring functionalization (i.e., using substituents in *ortho*, *meta* or *para* position). The scaffold choice benefitted from the availability of DNA-compatible reaction conditions, that had been optimized for uniform reactivity of different regioisomers using hundreds of different building blocks[23]. The new library (termed NF-DEL) comprised 670,752 members, yielded binders against a large set of different protein targets and produced hits with "antibody-like" binding properties. The stereocenter within the amino acid moiety and the regiochemistry of iodophenyl ring substitution had a strong impact for certain targets, leading to structurally compact ligands for several proteins of biomedical interest.

RESULTS

Library design and construction

Figure 1 depicts the strategy used for the synthesis of a DEL with 670,752 members. A scaffold based on 2-azido-3-iodophenylpropionate structures, featuring an iodine in *ortho*, *meta* or *para* position, was used for stepwise library construction. Scaffolds were coupled

to a universal amino-tagged 14-mer oligonucleotide by amide bond formation, followed by functionalization of the azido moiety by copper-catalyzed alkyne-azide cyclization with terminal alkyne derivatives or by Staudinger reduction and subsequent amide bond formation with a set of carboxylic acids. The resulting conjugates were HPLC purified prior to an encoding step, featuring a splint ligation (Building Blocks A; red code in the Figure)[23,27,36]. The chemical transformation in this first reaction step and, simultaneously, the regiochemistry of the iodophenyl moiety was encoded using 612 oligonucleotides [3 (regioisomers) x 204 (building blocks); Figure 1; Supplementary Figures 6 and 7].

The stereocenter within the azido-acid moiety was not encoded at this step, as the binding affinity of the different stereoisomers can be determined at the hit validation stage. The resulting conjugates were then mixed in equimolar amounts, split into 548 vials and used for a subsequent transformation step, using Suzuki coupling or Sonogashira reactions. The experimental conditions for these transformations had previously been investigated by us[37] and by other groups[38–43] and have further been optimized [Supplementary Figure 13]. In analogy to the first step, the chemical structure of the second set of building blocks was encoded by splint ligation (Building Blocks B; blue code in the Figure). Conjugates were then pooled, purified by RP-HPLC and used for selection in either single-stranded or double-stranded DNA format, using recently described procedures[44].

Library selections and hit validation

Figure 2 shows the selection results against carbonic anhydrase IX (CAIX), a tumor-associated membrane protein that can be recognized by aromatic sulfonamides[16,23,27,30,45,46]. The fingerprints of the library before selection or after selections (performed in duplicate) are displayed in Figure 2a, using a three-dimensional representation, in which two axes correspond to the identity of building blocks A and B, while the third axis indicates the number of sequence counts observed for individual molecules. Sequence counts are also indicated by a color code. A cut-off value (indicated in all Figures) was used in order to restrict the display of selection results only for those molecules which had reached a minimal level of sequence counts. While the distribution of sequence counts was homogeneous in the unselected library, distinctive lines of enriched compounds could be seen after CAIX selection [Figure 2a]. Fingerprints from replicate selections were remarkably reproducible and led to the identification of certain building block combinations as preferential CAIX binders.

We resynthesized molecules based on the **A160**/**B475** combination on solid phase, using a three amino acid linker [HO-βAla-Asp-Lys-NH_2; **LH** in Figure 2] at the position which was originally occupied by the DNA tag within the library. The charged peptide linker was chosen in order to contribute to an increased compound solubility in water. The resulting amine derivatives (e.g. compounds **7**, **9** and **11**) were reacted with fluorescein isothiocyanate (FITC), giving rise to thiourea products that could be purified by HPLC and characterized. Fluorescence polarization measurements performed at increasing concentrations of CAIX, revealed a dissociation constant of 8.8±0.3 nM and 7.2±0.3 nM for compounds **8** [**(*S*)-Phe/(*R*,*S*)A160/B475**] and **10** [**(*R*)-Phe/(*R*,*S*)A160/B475**] [Figure 2b], respectively. In comparison to compound **12** (**B475**, a derivative of triazol-benzenesulfonamide) and 4-

sulfamoylbenzoic acid (**p-SABA**)[47], the dissociation constants were improved up to thirty-fold [Supplementary Table 6]. Protein binding was also confirmed using a modified enzyme-linked immunosorbent assay (ELISA) procedure, featuring the binding of the fluorescein-conjugated molecules to immobilized protein on a solid support, followed by washing steps and incubation with anti-fluorescein antibody reagents[48]. ELISA tests are normally performed using monoclonal antibodies as primary reagents, but fluorescein-conjugated small organic molecules exhibited an "antibody-like" behavior in this assay [Figure 2b]. The binding of compound **8** [**(*R*)-Phe/(*R,S*)A160/B475**] and compound **10** [**(*S*)-Phe/(*R,S*)A160/B475**] to CAIX on CAIX-positive tumor cell lines (SK-RC-52) was also confirmed by fluorescence-activated cell sorting [Figure 2c].

Encouraged by the selection of high-affinity CAIX ligands, we studied whether fluorescein-conjugated derivatives of compounds **8** and **10** could be used as small molecule "adaptors" for conditional tumor cell killing by universal chimeric antigen receptor T (UniCAR-T) cells[35], and for tumor targeting applications. Human CAR-T cells, engineered to display a scFv antibody fragment specific to fluorescein, efficiently killed SK-RC-52 renal cell carcinomas only in the presence of the "bridge" molecules **8** and **10** [Figure 2d and 2e]. In a separate experiment, compound **8** was injected into tumor-bearing mice, which were sacrificed 60 minutes later and whose tissues were analyzed using fluorescence microscopy techniques[30]. A preferential uptake of compound **8** in tumor sections, compared to normal organs, was clearly visible [Figure 2f].

Figure 3 shows the results of DEL selections against cyclic-AMP response element binding protein (CREB) binding protein (CREBBP) bromodomain, a transcriptional co-regulator that is involved in many key intracellular processes[49–52].

Selection fingerprints (represented in Figure 3a both in 3D and 2D rendering) led to the identification of **A130/B99** as preferential binders. Resynthesis and characterization of these molecules (**13** and **14**) as FITC derivatives revealed that the (*S*) enantiomer bound to the cognate tag (compound **13**) with a Kd = 0.91±0.06 μM, while the corresponding (*R*) stereoisomer (compound **14**) exhibited a substantially reduced binding affinity (Kd = 6.0±0.7 μM) [Figure 3b]. These findings were confirmed by small molecule ELISA [Figure 3c]. Moreover, compounds **13** and **14** exhibited a substantially reduced interaction with the bromodomain-containing proteins BRD4(1) and BPTF, suggesting a preferential interaction with the CREBBP bromodomain [Figure 3b].

We also performed selections against variants of phosphoinositide 3-kinase (p110α/p85α **PI3K**)[53–56], in order to learn whether binders could be found that discriminate between the wildtype enzyme and a mutant form (e.g., His1047→Arg) frequently found in tumor cells[56,57]. A comparative inspection of selection fingerprints revealed a preferential enrichment of **A110/B489** (*para* regioisomer) against the wildtype protein and of **A110/B319** against the mutant [Figure 4a].

Affinity measurements showed a Kd = 126±2 nM for the (*R*) stereoisomer (compound **17**) and Kd = 306±8 nM for the (*S*) enantiomer (compound **16**) of **A110/B489** towards the wildtype protein [Figure 4b]. Importantly, the **A110/B319** combination (compound **22**)

exhibited a Kd = 185±20 nM for **H1047R-PI3K**, with a 20-fold selectivity compared to the wildtype protein [Figure 4c,d]. Additional combinations of building blocks (e.g., **A110/B157**) were enriched against the mutant protein and displayed an increased potency in ELISA [Figure 4c,d]. These results were reproducible in triplicate selection experiments [Supplementary Figure 21].

Selections were also performed against cancer targets, including murine and human extradomain D of tenascin-C (a tumor-associated antigen which is abundantly found in the neoplastic extracellular matrix[58]) [Figure 5a,b], the Leu27→Glu mutant of human CtIP (a multifunctional protein involved in the repair of DNA double-strand breaks[59]) [Figure 5c] and urokinase-type plasminogen activator (uPA, a strong prognostic marker of poor outcome in metastatic breast cancer[60]) [Figure 5d]. The Leu27→Glu mutation abrogates CtIP tetramer assembly, leading to strong defects in DNA end resection and homologous recombination[61]. Selection fingerprints were displayed in two-dimensional format, featuring the building blocks in the two dimensions and sequence counts as color code[44]. A preferential enrichment of **A481/B335** was observed in the tenascin-C selections, both for the murine and the human antigen, which share a 90% sequence identity [Figure 5a,b]. Compounds with apparent Kd values in the 10–30 μM range were identified [Figure 5a,b, Supplementary Figure 22 and Supplementary table 6]. Connecting two moieties of **(*S*)-Phe/A481/B335** through a β-alanine/β-alanine/lysine linker led to the dimeric compound **26,** which bound to human tenascin C, displaying an apparent Kd value of 1.7 ± 0.1 μM. Interesting binders directed against L27E-CtIP and uPA could further be identified and confirmed by ELISA after resynthesis [Figure 5c,d].

DISCUSSION

A regio- and stereo-defined DEL has been synthesized, which has been screened against multiple protein targets and has produced specific hits, often with dissociation constants in the submicromolar range. Ligands exhibited antibody-like binding properties, as target recognition could be confirmed in all cases using an adapted ELISA methodology[62] with human monoclonal IgG1 antibody bearing the anti-fluorescein variable heavy and light chains previously described[48].

We tested our library by performing selections against biomedically relevant proteins, some of which belonged to classes which are considered to be “difficult to drug” using small molecule ligands (e.g., transcription factors, protein-protein interactions). We found ligands that discriminated between closely-related protein targets. The discovery of selective binders **22** and **23**, with a 20-fold higher affinity towards the H1047R mutant of p110α in the p110α/p85α **PI3K** complex, may be of practical relevance since the mutation is frequently found in cancer and is associated with PI3K/AKT/mTOR signaling activation[63,64]. Similarly, **13** and **14** recognized CREBBP bromodomain but not the closely-related bromodomains of BRD4(1) and BPTF. CREBBP malfunctioning may cause mental diseases and growth deficiencies such as Rubinstein-Taybi Syndrome 1 (RSTS1)[65] and Menke-Hennekam Syndrome 1 (MKHK1)[66] as well as the growth of some types of cancer[49,67–69]. For therapeutic applications, a high CREBBP selectivity over other bromodomain-containing proteins is desirable[52,70].

For certain targets, the regiochemistry of iodophenylalanine modification and the chiral center of this amino acid contributed to the experimentally observed enrichment factors and affinity constants. For example, PI3K binders based on the **A110**-**B489** combination revealed that the *para* regioisomers had >20-fold improved affinity, while a 2.5-fold difference in Kd values between the R and S stereoisomers of the *para* derivative was observed [Figure 4].

Small-molecules used for *in vivo* tumor-targeting applications have often been derived from naturally-occurring compounds. For example, folate derivatives have been used to target folate receptors on ovarian cancer and other types of tumor cells[33], while somatostatin analogues have been used to target somatostatin receptors overexpressed in neuroendocrine tumors[71,72]. “Drugs of the future” for targeted cancer therapy should not be limited to those cancer entities for which natural ligands exist. Both the discovery of accessible tumor markers[73–75] and the facile identification of small organic ligands[76] will be crucially important.

Small organic ligands for tumor-associated antigens can serve as versatile building blocks for the development of innovative biomedical strategies. This concept is well exemplified by the use of fluorescein conjugates in UniCAR-T cell technology. Conventional chimeric antigen receptor (CAR) T cells have been used to treat certain hematological malignancies, leading to durable complete responses[77]. However, CAR-T cells (which display anti-tumor antibodies on their surface) exhibit a constitutive biocidal activity, that cannot easily be switched off and which may lead to *in vivo* toxicity (e.g., B cell aplasia in anti-CD19 CAR-T therapeutics)[77]. UniCAR-T cells kill tumor cells only in the presence of suitable fluorescein-conjugates, which act as a “bridge” between the engineered T cell and the cancer cell. When the fluorescein-conjugated adaptor has cleared from the body (e.g., by renal clearance), the UniCAR-T cell loses its biocidal activity, which can be reactivated at a later time point by a subsequent administration of the adaptor molecule[78]. Compared to antibodies small organic ligands can reach the target rapidly *in vivo*, and also clear from circulation within minutes after intravenous injection[30,79–82]. Small organic ligand derivatives (e.g., fluorescein conjugates) might outperform antibodies for UniCAR-T cell therapy[33,34,78]. CAIX ligands are ideally suited for the *in vivo* targeting [Figure 2f] of renal cell carcinomas[30,31], but other targets expressed on a broader set of cancer entities may be preferable for practical applications. For example, tenascin-C splice isoforms [Figure 5a,b] are found in the majority of solid tumors, lymphomas and in the bone marrow of acute leukemias, while being virtually undetectable in normal adult tissues[83,84].

In our laboratory, we have built DELs for the last 17 years, and the NF-DEL has proven to be one of the most productive sources of protein binding specificities, despite containing only 670,752 compounds. The library had a high purity, as reactions with excellent conversion yields were used. Moreover, the compact structures generated by Suzuki or Sonogashira coupling enabled the regio- and stereo-defined projection of functional groups towards the cognate target protein. Collectively, this work provides additional evidence for the potential of DEL technology as a versatile and convenient source of small molecule ligands for important therapeutic targets. Compared to conventional collections of chemical compounds for high-throughput screening, which may contain up to one million molecules

and can cost over a billion dollars[2,3], a library such as the one described contains a similar number of compounds, does not require expensive logistics, and can be productively screened against multiple protein targets in a relatively short timeframe.

METHODS

Detailed methods, synthetic procedures and characterization of compounds are described in the Supplementary Information.

Library synthesis.

Equimolar mixtures of scaffolds **1(*S*)** and **1(*R*)**, **2(*S*)** and **2(*R*)**, **3(*S*)** and **3(*R*)** **(**Supplementary Figure 1) were coupled to a universal 5' amino-modified oligonucleotide (5 μmol, 5'-C6-amino-*GGAGCTTCTGAATT*-3') using the 1-ethyl-3-(3-dimethylaminopropyl) carbodiimide (EDC) / *N*-hydroxysulfosuccinimide (S-NHS) method[1] (Supplementary Figure 2). The HPLC-purified derivatives **4 (*R*,*S*)**, **5 (*R*,*S*)** and **6 (*R*,*S*)** either were conjugated with 76 alkynes with a reported "on-DNA" CuAAC method[2] or reduced with tris(2-carboxyethyl)phosphine (TCEP, in TRIS pH=8 buffer, 40°C, 3h) and conjugated to additional 128 carboxylic acids[1]. The obtained 612 derivatives were individually purified by RP-HPLC. To each oligonucleotide-conjugates (5 nmol), 5′-phosphorylated-oligonucleotides (**code A**: 5'-*CTGTGTGCTG**XXXXXX**CGAGTCCCATGGCGC*-3' where **X** correspond to a variable region, 7.5 nmol), a 'splint' oligonucleotide (**s1**: 5'-*CAGCACACAGAATTCAGAAGCTCC*-3', 8.5 nmol) and NEB T4-ligase buffer were added. The reactions were heated for 5 minutes at 70 °C, cooled to room temperature followed by addition of T4 DNA ligase[3–5]. The ligation was kept at room temperature for 2 hours. The enzyme was deactivated by adding acetate buffer pH=4.7 and by heating at 70 °C for 5 minutes. The encoded derivatives were pooled, precipitated by ethanol and purified by RP-HPLC at 60°C (Supplementary Figures 6, 7 and 9). The step 1 of Library was split in 548 reaction vessels (1 nmol each) and coupled with 388 boronates and 160 alkynes through Suzuki and Sonogashira "on-DNA" cross-coupling[2] respectively (Supplementary Figures 12 and 13). The obtained derivatives (2 nmol) were precipitated and encoded by enzymatic ligation[3–5] using a 'splint' oligonucleotide (**s2**: 5'-*CGTCGATCCGGCGCCATGG*-3', 3.5 nmol) and an additional phosphorylated code (**code B**: 5'-*GGATCGACG**YYYYYYY**GCGTCAGGCAGC*-3' where **Y** correspond to a variable region, 3 nmol). The ligation products were pooled in equimolar amount and finally precipitated and purified (RP-HPLC, 60°C, Supplementary Figure 14) obtaining a final library containing 670'752 different combinations.

Affinity Selections.

The purified **NF-DEL** was screened in duplicate or in triplicate against the target proteins of interest as previously reported[6,7]. Additional details are reported in Chapter 5 of the Supplementary Information.

Hit re-synthesis.

The CREBBP binders were synthesized starting from (*S*)-2-amino-3-(4-iodophenyl)propanoic acid, (*R*)-2-amino-3-(4-iodophenyl)propanoic acid and (5-acetyl-2-

fluorophenyl)boronic acid. The Suzuki products were coupled with 4-bromopyridine-2-carboxylic acid and derivatized as α- L-lysine amide (Supplementary Information, Chapter 6.1). CAIX, wt-PI3K, H1047R-PI3K, uPA, hTNC, mTNC, CtIP binders and the negative control (**FluoL-NH_2**) have been synthesized on solid phase starting from Fmoc- L-Lys(Boc)-Wang resin in which L-Aspartic acid α-*tert*-butyl ester and β-alanine have been added as linker to the *iodo*-phenylalanine scaffolds. The building blocks A were added by amide coupling or CuAAC and the building blocks B by palladium-catalyzed Suzuki or Sonogashira cross-couplings. The final compounds were cleaved from the resin in acidic conditions, obtaining the fully-deprotected peptides (Supplementary Information, Chapter 6.2). The obtained lysine derivatives were further conjugated with fluorescein-5-isothiocyanate to obtain the desired FITC-labelled compounds (Supplementary Table 5).

FP measurements with FITC-labelled compounds.

The FITC-labelled compounds were diluted to a final concentration between 10 and 50 nM (5 μL) and incubated for 15 minutes in a black 384-well plate (Greiner small-volume, non-binding) with serial dilutions of protein (5 μL). The fluorophore was excited at 485 nm and the emission was measured at 535 nM on a Spectra Max Paradigm multimode plate reader (Molecular Devices). The experiments were performed in triplicate and the resulting data was fitted by Prism 7 ([Inhibitor] vs. response, Variable slope four parameters).

ELISA measurements with FITC-labelled compounds.

The protein (200 nM) was coated on F8 maxisorp (Thermo Scientific) plate overnight at 4 °C. The immobilized protein was incubated for 30 minutes in the dark with serial dilutions of FITC-labelled compound and an additional 30 minutes with human monoclonal IgG1 anti-fluorescein antibody[8]. After several washing steps, protein A-HRP (1 μg/mL) was added to each well and the non-bound protein was washed away. The substrate 3,3′,5,5′-tetramethylbenzidine (**TMB**) was added and developed in the dark for 1–5 minutes. The reaction was quenched by adding 50 μL of 1 M sulfuric acid. The absorbance was measured on a Spectra Max Paradigm multimode plate reader (Molecular Devices) at 620–650 nm and 450 nm. Additional details are reported in the Supplementary Information (Chapter 7.2).

UniCAR-T production and Killing assay.

The production of anti-fluorescein uniCAR-T and the killing assay against SK-RC-52 in presence of FITC-labelled small CAIX-binders were performed essentially as previously described[9,10], but using the vectors of Myburgh and colleagues for viral particle production and for cell transduction[11].

Ex-Vivo.

BALB/c nu/nu mice bearing established subcutaneous SK-RC-52 tumors (~400 mm^3) were injected intravenously with fluorescein-labelled compound **8** (50 nmol) dissolved in sterile PBS buffer pH 7.4 (100 μL). After 1 hour, the animals were sacrificed by CO_2 asphyxiation. The organs and tumors were extracted and flash-frozen in Neg-50 cryo medium (Thermo Fisher Scientific) with dry ice. The samples were cut into sections of 10 μm width and nuclear staining was performed with Fluorescence Mounting Medium containing DAPI

(Dako Omnis). All pictures were acquired on an Axioskop 2 fluorescence microscope (Zeiss).

Supplementary Material

Refer to Web version on PubMed Central for supplementary material.

Acknowledgments

Financial support by the ETH Zürich, the Swiss National Science Foundation (grant number 310030_182003/1), the European Research Council (ERC) under the European Union's Horizon 2020 research and innovation program (grant agreement 670603), the Federal Commission for Technology and Innovation (KTI, grant number 12803.1 VOUCH-LS), the Clinical Research Priority Program "ImmunoCure" of the University of Zurich to M.G.M and D.N, a University Research Priority Project Translational Cancer Research grant to R.M.; a Swiss Cancer Research grant to M.G.M. and D.N. (KFS-3846-02-2016) is gratefully acknowledged; the National Cancer Institute (R35 CA197582 to PKV) is gratefully acknowledged (TSRI ms. #29970). Work in the Sartori laboratory is supported by the Swiss National Science Foundation (grant number: 31003A_176161) and the Swiss Cancer Research Foundation (grant number: KFS-4702-02-2019). M.M. thanks the EPSRC Centre for Doctoral Training in Synthesis for Biology and Medicine (EP/L015838/1) for studentship support, supported by AstraZeneca, Diamond Light Source, Defence Science and Technology Laboratory, Evotec, GlaxoSmithKline, Janssen, Novartis, Pfizer, Syngenta, Takeda, UCB, and Vertex. S.J.C. thanks St Hugh's College, Oxford, for research funding. We further thank Davide Bianchi and Cressida Harvey for the synthesis of some of the molecules described in this manuscript and Marco Catalano for providing the anti-FITC antibody used in ELISA procedures. We thank Adriano Martinelli for his help with data evaluation and we are most grateful to Bernhard Pfeiffer for help with NMR measurements. We are also grateful to the Functional Genomics Center Zurich for help with high-throughput DNA sequencing. Instant JChem (ChemAxon) was used for structure and data management (http://www.chemaxon.com).

REFERENCES

1. Lerner RA & Brenner S. DNA-Encoded Compound Libraries as Open Source: A Powerful Pathway to New Drugs. Angew Chem Int Ed Engl 56, 1164–1165, doi:10.1002/anie.201612143 (2017). [PubMed: 28094476]
2. Neri D. & Lerner R. DNA-Encoded Chemical Libraries: A Selection System Based On Endowing Organic Compounds with Amplifiable Information. Annual Review of Biochemistry 87, 24 (2018).
3. Goodnow RA Jr., Dumelin CE & Keefe AD DNA-encoded chemistry: enabling the deeper sampling of chemical space. Nat Rev Drug Discov 16, 131–147, doi:10.1038/nrd.2016.213 (2017). [PubMed: 27932801]
4. Favalli N, Bassi G, Scheuermann J. & Neri D. DNA-encoded chemical libraries - achievements and remaining challenges. FEBS Lett 592, 2168–2180, doi:10.1002/1873-3468.13068 (2018). [PubMed: 29683493]
5. Dumelin CEet al.A portable albumin binder from a DNA-encoded chemical library. Angew Chem Int Ed Engl47, 3196–3201, doi:10.1002/anie.200704936 (2008). [PubMed: 18366035]
6. Franzini RM, Neri D. & Scheuermann J. DNA-encoded chemical libraries: advancing beyond conventional small-molecule libraries. Acc Chem Res 47, 1247–1255, doi:10.1021/ar400284t (2014). [PubMed: 24673190]
7. Liu R, Li X. & Lam KS Combinatorial chemistry in drug discovery. Curr Opin Chem Biol 38, 117–126, doi:10.1016/j.cbpa.2017.03.017 (2017). [PubMed: 28494316]
8. Zhu Z. & Cuozzo J. High-throughput affinity-based technologies for small-molecule drug discovery. J Biomol Screen 14, 1157–1164, doi:10.1177/1087057109350114 (2009). [PubMed: 19822881]
9. Zhao G, Huang Y, Zhou Y, Li Y. & Li X. Future challenges with DNA-encoded chemical libraries in the drug discovery domain. Expert Opinion on Drug Discovery 14, 19 (2019).
10. Brenner S. & Lerner RA Encoded combinatorial chemistry. Proceedings of the National Academy of Sciences of the United States of America 89, 5381–5383 (1992). [PubMed: 1608946]
11. Mannocci L. et al.High-throughput sequencing allows the identification of binding molecules isolated from DNA-encoded chemical libraries. Proceedings of the National Academy of Sciences105, 17670–17675 (2008).

12. Buller F. et al.High-throughput sequencing for the identification of binding molecules from DNA-encoded chemical libraries. Bioorg Med Chem Lett20, 4188–4192, doi:10.1016/j.bmcl.2010.05.053 (2010). [PubMed: 20538458]
13. Clark MAet al.Design, synthesis and selection of DNA-encoded small-molecule libraries. Nat Chem Biol5, 647–654, doi:10.1038/nchembio.211 (2009). [PubMed: 19648931]
14. Gartner ZJet al.DNA-Templated Organic Synthesis and Selection of a Library of Macrocycles. Science305, 1601 (2004). [PubMed: 15319493]
15. Melkko S, Scheuermann J, Dumelin CE & Neri D. Encoded self-assembling chemical libraries. Nat Biotechnol 22, 568–574, doi:10.1038/nbt961 (2004). [PubMed: 15097996]
16. Wichert M. et al.Dual-display of small molecules enables the discovery of ligand pairs and facilitates affinity maturation. Nat Chem7, 241–249, doi:10.1038/nchem.2158 (2015). [PubMed: 25698334]
17. Winter G, Griffiths AD, Hawkins RE & Hoogenboom HR MAKING ANTIBODIES BY PHAGE DISPLAY TECHNOLOGY. Annual Review of Immunology 12, 23 (1994).
18. Lerner RAet al.Antibodies from combinatorial libraries use functional receptor pleiotropism to regulate cell fates. Quarterly Reviews of Biophysics48, 389–394, doi:10.1017/s0033583515000049 (2015). [PubMed: 26537396]
19. Griffiths D, et al A. Isolation of high affinity human antibodies directly from large synthetic repertoires. EMBO J13, 16 (1994).
20. Machutta CAet al.Prioritizing multiple therapeutic targets in parallel using automated DNA-encoded library screening. Nat Commun8, 16081, doi:10.1038/ncomms16081 (2017). [PubMed: 28714473]
21. Eidam O. & Satz AL Analysis of the productivity of DNA encoded libraries. MedChemComm 7, 1323–1331, doi:10.1039/c6md00221h (2016).
22. Perelson AS & Oster GF Theoretical Studies of Clonal Selection: Minimal Antibody Repertoire Size and Reliability of Self-Non-self Discriminationt. J. theor. Biol. 81, 26 (1979).
23. Favalli N. et al.A DNA-encoded library of chemical compounds based on common scaffolding structures reveals the impact of ligand geometry on protein recognition. ChemMedChem13, 5 (2018).
24. Yuen LHet al.A Focused DNA-Encoded Chemical Library for the Discovery of Inhibitors of NAD(+)-Dependent Enzymes. J Am Chem Soc141, 5169–5181, doi:10.1021/jacs.8b08039 (2019). [PubMed: 30855951]
25. Lipinski CALead- and drug-like compounds: the rule-of-five revolution. Drug Discov Today Technol1, 337–341, doi:10.1016/j.ddtec.2004.11.007 (2004). [PubMed: 24981612]
26. Gerry CJ, Wawer MJ, Clemons PA & Schreiber SL DNA Barcoding a Complete Matrix of Stereoisomeric Small Molecules. J Am Chem Soc 141, 10225–10235, doi:10.1021/jacs.9b01203 (2019). [PubMed: 31184885]
27. Li Y. et al.Versatile protein recognition by the encoded display of multiple chemical elements on a constant macrocyclic scaffold. Nature Chemistry10, 441–448, doi:10.1038/s41557-018-0017-8 (2018).
28. Buller F. et al.Design and synthesis of a novel DNA-encoded chemical library using Diels-Alder cycloadditions. Bioorg Med Chem Lett18, 5926–5931, doi:10.1016/j.bmcl.2008.07.038 (2008). [PubMed: 18674904]
29. Franzini RM & Randolph C. Chemical Space of DNA-Encoded Libraries. J Med Chem 59, 6629–6644, doi:10.1021/acs.jmedchem.5b01874 (2016). [PubMed: 26914744]
30. Cazzamalli S, Dal Corso A, Widmayer F. & Neri D. Chemically Defined Antibody- and Small Molecule-Drug Conjugates for in Vivo Tumor Targeting Applications: A Comparative Analysis. J Am Chem Soc 140, 1617–1621, doi:10.1021/jacs.7b13361 (2018). [PubMed: 29342352]
31. Cazzamalli S, Corso AD & Neri D. Targeted Delivery of Cytotoxic Drugs: Challenges, Opportunities and New Developments. Chimia (Aarau) 71, 712–715, doi:10.2533/chimia.2017.712 (2017). [PubMed: 29070415]
32. Urbanska K. et al.A universal strategy for adoptive immunotherapy of cancer through use of a novel T-cell antigen receptor. Cancer Res72, 1844–1852, doi:10.1158/0008-5472.CAN-11-3890 (2012). [PubMed: 22315351]

33. Lee YGet al.Use of a Single CAR T Cell and Several Bispecific Adapters Facilitates Eradication of Multiple Antigenically Different Solid Tumors. Cancer Res79, 387–396, doi:10.1158/0008-5472.CAN-18-1834 (2019). [PubMed: 30482775]
34. Pellegrino Christianet al.Impact of ligand size and conjugation chemistry on the performance of universal chimeric antigen receptor T cells for tumor killing. Bioconjugate Chem. 31, 9 (2020).
35. Ma JSet al.Versatile strategy for controlling the specificity and activity of engineered T cells. Proc Natl Acad Sci U S A113, E450–458, doi:10.1073/pnas.1524193113 (2016). [PubMed: 26759368]
36. Litovchick A. et al.Encoded Library Synthesis Using Chemical Ligation and the Discovery of sEH Inhibitors from a 334-Million Member Library. Sci Rep5, 10916, doi:10.1038/srep10916 (2015). [PubMed: 26061191]
37. Favalli N, Bassi G, Zanetti T, Scheuermann J. & Neri D. Screening of Three Transition Metal Mediated Reactions Compatible with DNA Encoded Chemical Libraries. Helvetica Chimica Acta 102, doi:10.1002/hlca.201900033 (2019).
38. Satz ALet al.DNA Compatible Multistep Synthesis and Applications to DNA Encoded Libraries. Bioconjug Chem26, 1623–1632, doi:10.1021/acs.bioconjchem.5b00239 (2015). [PubMed: 26024553]
39. de Pedro Beato E. et al.Mild and Efficient Palladium-mediated C-N Cross-Coupling Reaction between DNA-conjugated Aryl Bromides and Aromatic Amines. ACS Comb Sci, doi:10.1021/acscombsci.8b00142 (2019).
40. Li JY & Huang H. Development of DNA-Compatible Suzuki-Miyaura Reaction in Aqueous Media. Bioconjug Chem 29, 3841–3846, doi:10.1021/acs.bioconjchem.8b00676 (2018). [PubMed: 30339361]
41. Hervé G. & Len C. Heck and Sonogashira couplings in aqueous media – application to unprotected nucleosides and nucleotides. Sustainable Chemical Processes 3, doi:10.1186/s40508-015-0029-2 (2015).
42. Ding Y. & Clark MA Robust Suzuki–Miyaura Cross-Coupling on DNA-Linked Substrates. ACS Combinatorial Science 17, 1–4, doi:10.1021/co5001037 (2014). [PubMed: 25459065]
43. Ding Y, DeLorey JL & Clark MA Novel Catalyst System for Suzuki-Miyaura Coupling of Challenging DNA-Linked Aryl Chlorides. Bioconjug Chem 27, 2597–2600, doi:10.1021/acs.bioconjchem.6b00541 (2016). [PubMed: 27704784]
44. Bassi G. et al.Comparative evaluation of DNA-encoded chemical selections performed using DNA in single-stranded or double-stranded format. Biochem Biophys Res Commun533, 223–229, doi:10.1016/j.bbrc.2020.04.035 (2020). [PubMed: 32386812]
45. Supuran CTCarbonic anhydrases: novel therapeutic applications for inhibitors and activators. Nat Rev Drug Discov7, 168–181 (2008). [PubMed: 18167490]
46. Alterio V, Esposito D, Monti SM, Supuran CT & De Simone G. Crystal structure of the human carbonic anhydrase II adduct with 1-(4-sulfamoylphenyl-ethyl)-2,4,6-triphenylpyridinium perchlorate, a membrane-impermeant, isoform selective inhibitor. J Enzyme Inhib Med Chem 33, 151–157, doi:10.1080/14756366.2017.1405263 (2018). [PubMed: 29199489]
47. Sannino A. et al.Quantitative Assessment of Affinity Selection Performance by Using DNA-Encoded Chemical Libraries. ChemBioChem20, 7, doi:10.1002/ (2019). [PubMed: 30320963]
48. Midelfort KSet al.Substantial energetic improvement with minimal structural perturbation in a high affinity mutant antibody. J Mol Biol343, 685–701, doi:10.1016/j.jmb.2004.08.019 (2004). [PubMed: 15465055]
49. Breen ME & Mapp AK Modulating the masters: chemical tools to dissect CBP and p300 function. Curr Opin Chem Biol 45, 195–203, doi:10.1016/j.cbpa.2018.06.005 (2018). [PubMed: 30025258]
50. Rooney TPet al.A series of potent CREBBP bromodomain ligands reveals an induced-fit pocket stabilized by a cation-pi interaction. Angew Chem Int Ed Engl53, 6126–6130, doi:10.1002/anie.201402750 (2014). [PubMed: 24821300]
51. Schiedel M. & Conway SJ Small molecules as tools to study the chemical epigenetics of lysine acetylation. Curr Opin Chem Biol 45, 166–178, doi:10.1016/j.cbpa.2018.06.015 (2018). [PubMed: 29958150]

52. Brand M. et al.Controlling Intramolecular Interactions in the Design of Selective, High-Affinity, Ligands for the CREBBP Bromodomain. ChemRxiv. Preprint 10.26434/chemrxiv.12081999.v1 (2020).
53. Huang CHThe structure of a human p110alpha/p85alpha complex elucidates the effects of oncogenic PI3Kalpha mutations. Science318, 1744–1748, doi:10.1126/science.1150799 (2007). [PubMed: 18079394]
54. Katso R. et al.CELLULAR FUNCTION OF PHOSPHOINOSITIDE 3-KINASES: Implications for Development, Immunity, Homeostasis, and Cancer. Annu. Rev. Cell Dev. Biol. 17, 61 (2001).
55. Zhao L. & Vogt PK Class I PI3K in oncogenic cellular transformation. Oncogene 27, 5486–5496, doi:10.1038/onc.2008.244 (2008). [PubMed: 18794883]
56. Samuels Y. et al.High Frequency of Mutations of the PIK3CA Gene in Human Cancers. SCIENCE304, 1 (2004).
57. Miller MSet al.Identification of allosteric binding sites for PI3Kalpha oncogenic mutant specific inhibitor design. Bioorg Med Chem25, 1481–1486, doi:10.1016/j.bmc.2017.01.012 (2017). [PubMed: 28129991]
58. Brack SS, Silacci M, Birchler M. & Neri D. Tumor-targeting properties of novel antibodies specific to the large isoform of tenascin-C. Clin Cancer Res 12, 3200–3208, doi:10.1158/1078-0432.CCR-05-2804 (2006). [PubMed: 16707621]
59. Sartori AAet al.Human CtIP promotes DNA end resection. Nature450, 509–514, doi:10.1038/nature06337 (2007). [PubMed: 17965729]
60. Kubala MH & DeClerck YA The plasminogen activator inhibitor-1 paradox in cancer: a mechanistic understanding. Cancer Metastasis Rev 38, 483–492, doi:10.1007/s10555-019-09806-4 (2019). [PubMed: 31734763]
61. Davies ORet al.CtIP tetramer assembly is required for DNA-end resection and repair. Nat Struct Mol Biol22, 150–157, doi:10.1038/nsmb.2937 (2015). [PubMed: 25558984]
62. Prati L, Bigatti M, Donckele EJ, Neri D. & Samain F. On-DNA hit validation methodologies for ligands identified from DNA-encoded chemical libraries. Biochem Biophys Res Commun 533, 235–240, doi:10.1016/j.bbrc.2020.04.030 (2020). [PubMed: 32362331]
63. Yang H. et al.Discovery of a Potent Class of PI3Kalpha Inhibitors with Unique Binding Mode via Encoded Library Technology (ELT). ACS Med Chem Lett6, 531–536, doi:10.1021/acsmedchemlett.5b00025 (2015). [PubMed: 26005528]
64. Janku F. et al.PIK3CA mutation H1047R is associated with response to PI3K/AKT/mTOR signaling pathway inhibitors in early-phase clinical trials. Cancer Res73, 276–284, doi:10.1158/0008-5472.CAN-12-1726 (2013). [PubMed: 23066039]
65. Alari V. et al.Generation of three iPSC lines (IAIi002, IAIi004, IAIi003) from Rubinstein-Taybi syndrome 1 patients carrying CREBBP non sense c.4435G>T, p.(Gly1479*) and c.3474G>A, p.(Trp1158*) and missense c.4627G>T, p.(Asp1543Tyr) mutations. Stem Cell Research40, doi:10.1016/j.scr.2019.101553 (2019).
66. Banka S. et al.Genotype-phenotype specificity in Menke-Hennekam syndrome caused by missense variants in exon 30 or 31 of CREBBP. Am J Med Genet A179, 1058–1062, doi:10.1002/ajmg.a.61131 (2019). [PubMed: 30892814]
67. Steven A. & Seliger B. Control of CREB expression in tumors: from molecular mechanisms and signal transduction pathways to therapeutic target. Oncotarget 7, 12 (2015).
68. Wang H, Xu J, Lazarovici P, Quirion R. & Zheng W. cAMP Response Element-Binding Protein (CREB): A Possible Signaling Molecule Link in the Pathophysiology of Schizophrenia. Front Mol Neurosci 11, 255, doi:10.3389/fnmol.2018.00255 (2018). [PubMed: 30214393]
69. Belmaker RH & Agam G. Major Depressive Disorder. The New England Journal of Medicine 358, 14 (2008).
70. Schiedel M. Chemical Epigenetics: The Impact of Chemical and Chemical Biology Techniques on Bromodomain Target Validation. Angew Chem Int Ed Engl58, 17930–17952, doi:10.1002/anie.201812164 (2019). [PubMed: 30633431]
71. Reubi JC, Mäcke HR & Krenning EP Candidates for Peptide Receptor Radiotherapy Today and in the Future. J Nucl Med 46, 9 (2005).

72. Reubi JCet al.SST3-selective potent peptidic somatostatin receptor antagonists. Proc Natl Acad Sci U S A97, 13973–13978, doi:10.1073/pnas.250483897 (2000). [PubMed: 11095748]
73. Rybak JNet al.In vivo protein biotinylation for identification of organ-specific antigens accessible from the vasculature. Nat Methods2, 291–298, doi:10.1038/nmeth745 (2005). [PubMed: 15782212]
74. Bodenmiller B. et al.Multiplexed mass cytometry profiling of cellular states perturbed by small-molecule regulators. Nat Biotechnol30, 858–867, doi:10.1038/nbt.2317 (2012). [PubMed: 22902532]
75. Parker CGet al.Ligand and Target Discovery by Fragment-Based Screening in Human Cells. Cell168, 527–541 e529, doi:10.1016/j.cell.2016.12.029 (2017). [PubMed: 28111073]
76. Krall N, Scheuermann J. & Neri D. Small targeted cytotoxics: current state and promises from DNA-encoded chemical libraries. Angew Chem Int Ed Engl 52, 1384–1402, doi:10.1002/anie.201204631 (2013). [PubMed: 23296451]
77. Maude SLet al.Tisagenlecleucel in Children and Young Adults with B-Cell Lymphoblastic Leukemia. N Engl J Med378, 439–448, doi:10.1056/NEJMoa1709866 (2018). [PubMed: 29385370]
78. Lee YGet al.Regulation of CAR T cell-mediated cytokine release syndrome-like toxicity using low molecular weight adapters. Nat Commun10, 2681, doi:10.1038/s41467-019-10565-7 (2019). [PubMed: 31213606]
79. Krall N. et al.A small-molecule drug conjugate for the treatment of carbonic anhydrase IX expressing tumors. Angew Chem Int Ed Engl53, 4231–4235, doi:10.1002/anie.201310709 (2014). [PubMed: 24623670]
80. Lindner T. et al.Development of Quinoline-Based Theranostic Ligands for the Targeting of Fibroblast Activation Protein. J Nucl Med59, 1415–1422, doi:10.2967/jnumed.118.210443 (2018). [PubMed: 29626119]
81. Loktev A. et al.Development of Fibroblast Activation Protein-Targeted Radiotracers with Improved Tumor Retention. J Nucl Med60, 1421–1429, doi:10.2967/jnumed.118.224469 (2019). [PubMed: 30850501]
82. Giesel FLet al.68Ga-FAPI PET/CT: Biodistribution and Preliminary Dosimetry Estimate of 2 DOTA-Containing FAP-Targeting Agents in Patients with Various Cancers. Journal of Nuclear Medicine60, 386–392, doi:10.2967/jnumed.118.215913 (2019). [PubMed: 30072500]
83. Silacci M. et al.Human monoclonal antibodies to domain C of tenascin-C selectively target solid tumors in vivo. Protein Eng Des Sel19, 471–478, doi:10.1093/protein/gzl033 (2006). [PubMed: 16928692]
84. Schliemann C. et al.Three clinical-stage tumor targeting antibodies reveal differential expression of oncofetal fibronectin and tenascin-C isoforms in human lymphoma. Leuk Res33, 1718–1722, doi:10.1016/j.leukres.2009.06.025 (2009). [PubMed: 19625084]
85. Li Y. et al.Optimized Reaction Conditions for Amide Bond Formation in DNA-Encoded Combinatorial Libraries. ACS Comb Sci18, 438–443, doi:10.1021/acscombsci.6b00058 (2016). [PubMed: 27314981]
86. Franzini RMet al.Identification of structure-activity relationships from screening a structurally compact DNA-encoded chemical library. Angew Chem Int Ed Engl54, 3927–3931, doi:10.1002/anie.201410736 (2015). [PubMed: 25650139]
87. Decurtins W. Automated screening for small organic ligands using DNA-encoded chemical libraries. Nat Protoc11, 764–780, doi:10.1038/nprot.2016.039 (2016). [PubMed: 26985574]
88. Myburgh R. et al.Anti-human CD117 CAR T-cells efficiently eliminate healthy and malignant CD117-expressing hematopoietic cells. Leukemia34, 2688–2703, doi:10.1038/s41375-020-0818-9 (2020). [PubMed: 32358567]

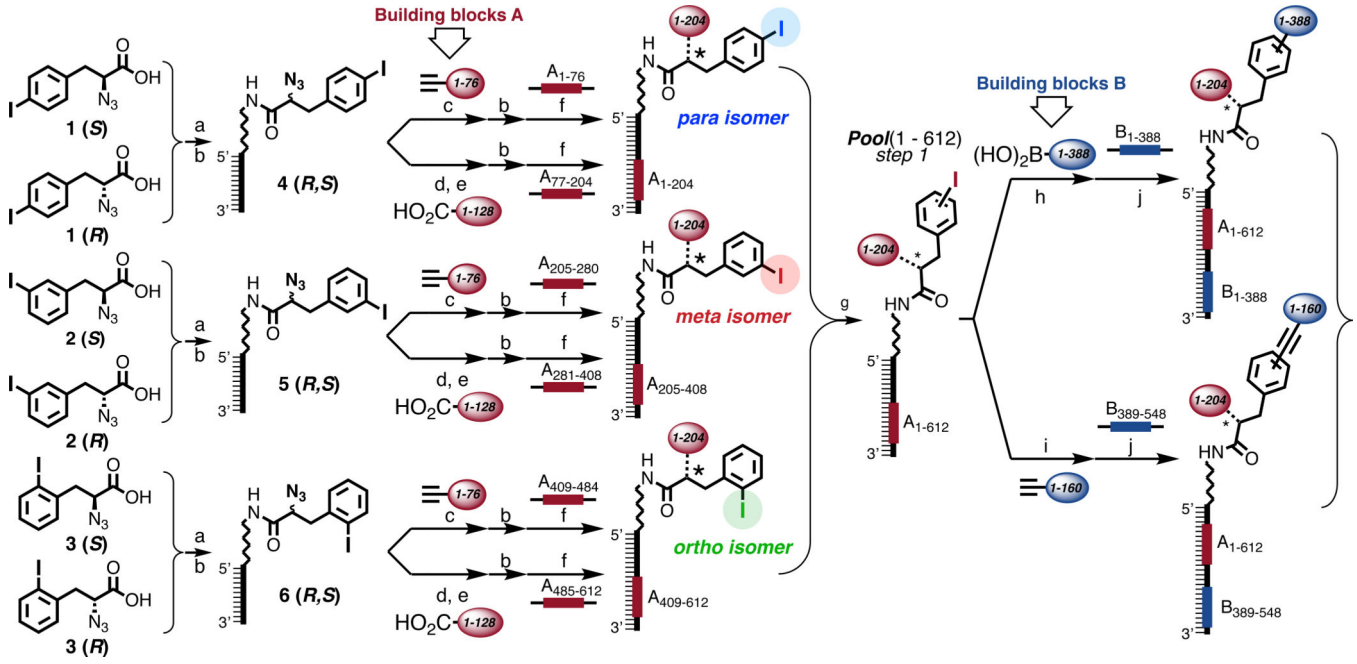

Figure 1 |. Library design, synthesis and encoding.

Schematic representation of the strategy used for library synthesis, using regio- and stereoisomers of 2-azido-3-iodophenylpropionic acid. The chemical building blocks A and B and the corresponding encoding DNA portions are color-coded in red and blue, respectively. The first set of building blocks was conjugated to the central scaffold through a triazole ring or amide bond (*), the second set of building blocks was connected by either Suzuki- or Sonogashira coupling. **a**, EDC, S-NHS, DIPEA, r.t., 30', 5'-C6-amino-GGAGCTTCTGAATT in TEA buffer (pH=10), 37 °C, 6h. **b**, RP-HPLC purification. **c**, CuAAC on-DNA reaction[37] **d**, TCEP, TRIS buffer pH=7, 40 °C, 3h, RP-HPLC purification. **e**, on-DNA amide bond formation[85]. **f**, adaptor 5'-CAGCACACAGAATTCAGAAGCTCC-3', ligase buffer, T4 DNA-ligase. **g**, RP-HPLC purification at 60°C. **h**, $Pd(OAc)_2$, TPPTS, 200 mM Na_2CO_3, 60°C, 3h[37]. **i**, $Pd(OAc)_2$, TPPTS, $CuSO_4$, Ascorbate, 200 mM Na_2CO_3, 70°C, 2h[37]. **j**, adaptor 5'-CGTCGATCCGGCGCCATGG-3', ligase buffer, T4 DNA-ligase. See Chapter 4 and 8 of the Supplementary Information for exact structures and detailed conditions.

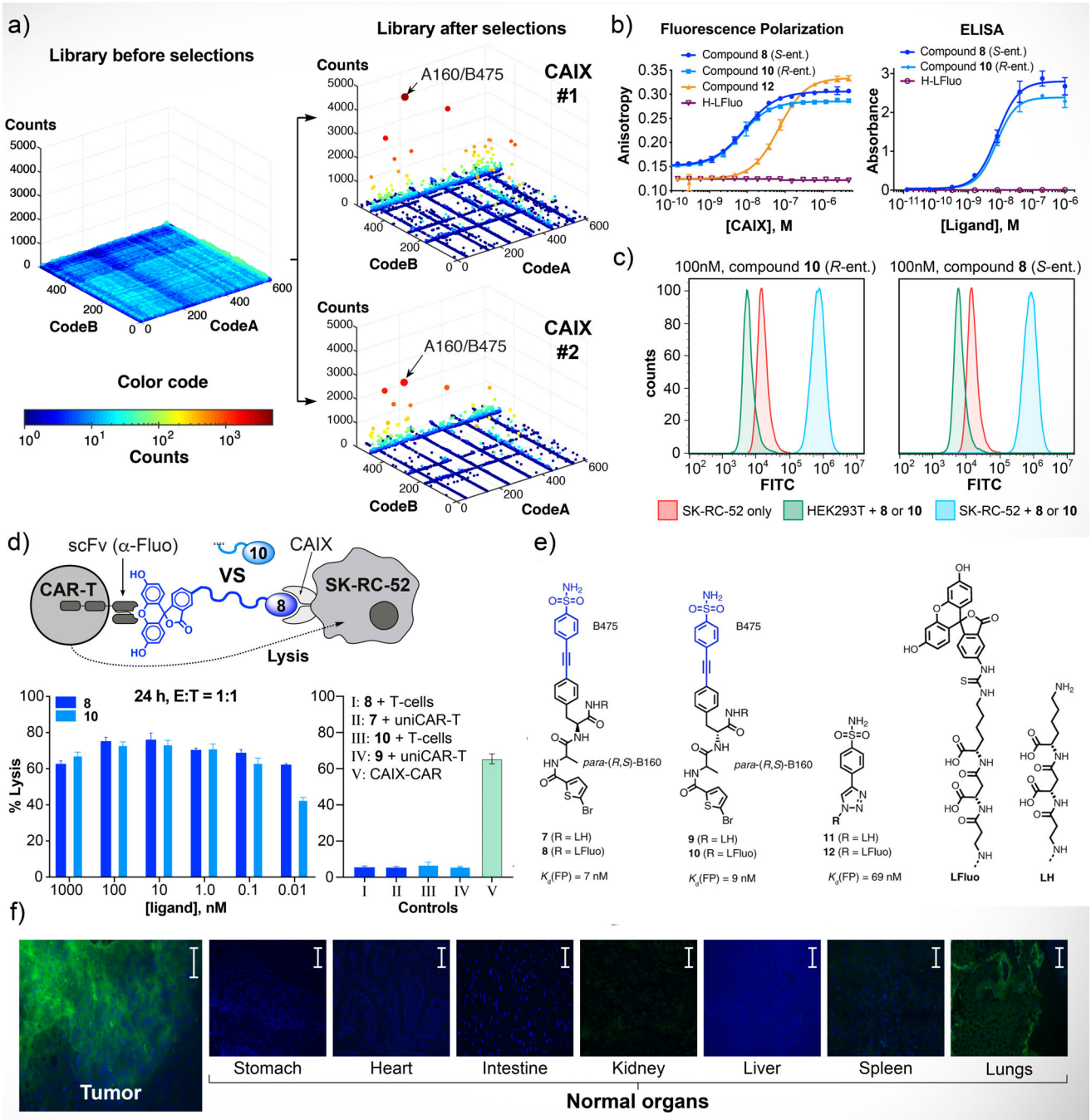

Figure 2 |. Selection against carbonic anhydrase IX, hit validation and conversion of ligands to CAR-T cell activators.

a, NF-DEL high-throughput DNA sequencing results represented as three-dimensional fingerprints before and after selections against CAIX. The x and y axes represent the two building blocks while the color heat map and z-axis correspond to the DNA sequence counts. Selections were performed in triplicate (see Supplementary Figure 21). In order to show reproducibility of selection results, two CAIX prints are shown in this Figure. Cut-off values equal to 20 (for CAIX selection #1) and 15 (for CAIX selection #2) were applied to

the fingerprints. No cut-off was applied for the naïve library fingerprint. The most enriched combination is indicated with an arrow (average EF=23±5 × 10^2). For the calculation of enrichment factors (EF) see Supplementary Tables 2,3 and **Equation 1** (S29). **b**, off-DNA affinity measurements of selected compounds by FP and small-molecule ELISA, see also Supplementary Table 6. Error bars indicate standard deviation of three measurements. **c**, FACS with **8** and **10** on SK-RC-52 cells (renal cell carcinoma, in blue), on HEK293T (human embryonic kidney cells, control, in green), on SK-RC-52 cells alone (renal cell carcinoma, control, in red). **d**, Schematic representation of the immunological synapse of a fluorescein-specific universal CAR-T cell with a CAIX-presenting SK-RC-52 tumor cell, established by cross-linking the cells with the heterobifunctional crosslinker (blue). Killing was monitored after 24 h. % SK-RC-52 lysis is given as a function of ligand **8** (dark blue) and **10** (light blue) concentration. % SK-RC-52 lysis is also given for controls I-IV and the functional combination V(anti CAIX CAR-T). Error bars indicate standard deviation of three measurements **e**, Chemical structures of compounds **7**, **8**, **9**, **10**, **11**, **12** and of tripeptide linker (**LH, LFluo**). **f**, Evaluation of the tumor-targeting performance of compound **8** after *i.v.* administration for human SK-RC-52 xenografted in mice, using *ex vivo* immunofluorescence detection of the fluorescein moiety. Images were taken 60 min after intravenous injection of 65 μg of compound **8** (green = ligand, blue = DAPI staining. Scale bar = 100 μm).

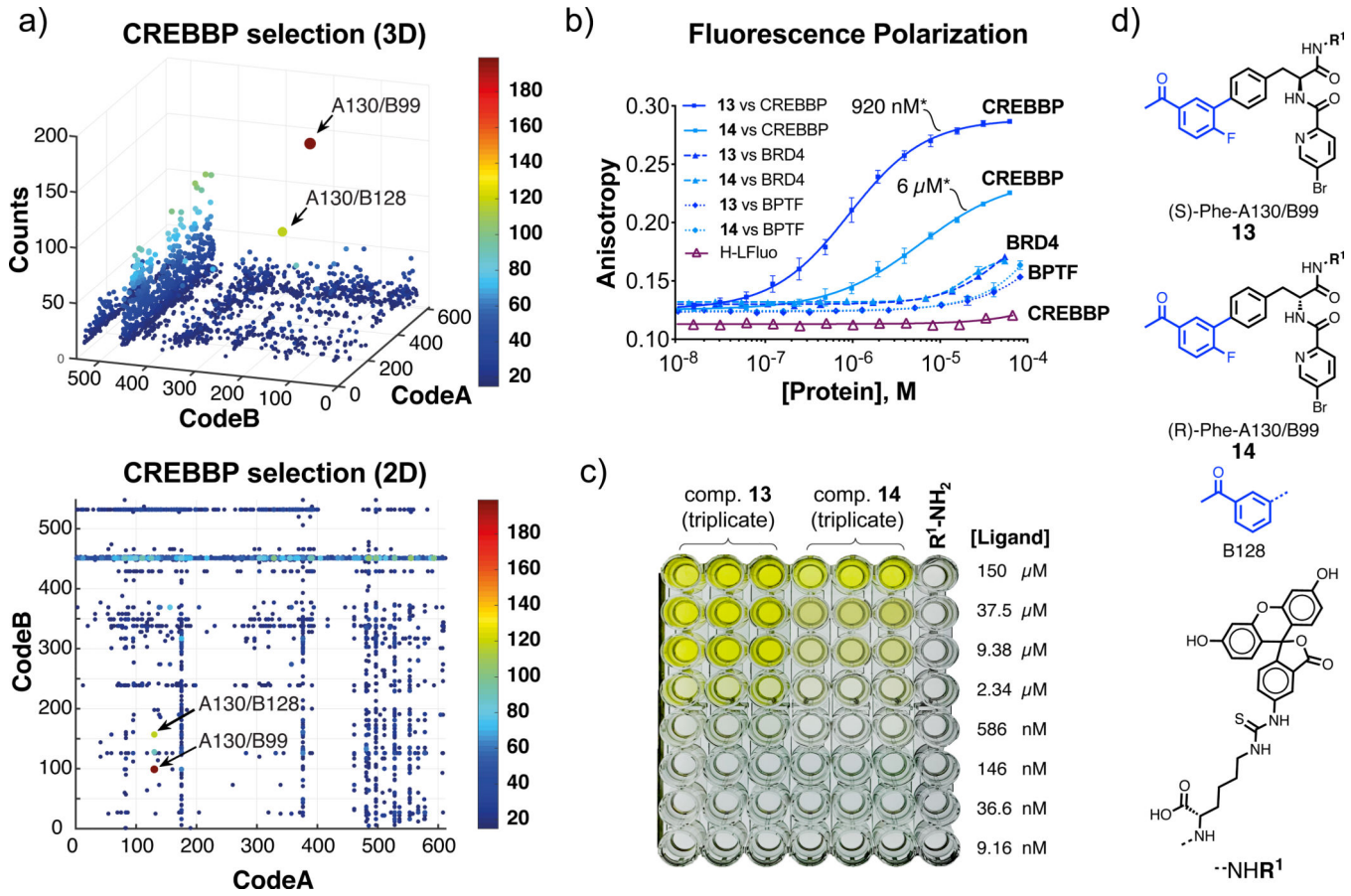

Figure 3 |. Selection against CREBBP bromodomain, hit validation and selectivity determination.

a, Fingerprint of a CREBBP bromodomain selection plotted in 3D and 2D representation, respectively. The x and y axes represent the two building blocks while the color heat map and z-axis correspond to the DNA sequence counts. A cut-off value equal to 15 was applied to fingerprints. Combinations **A130/B99** and **A130/B128** were preferentially enriched ($EF_{A130/B99}$=149±16 and $EF_{A130/B128}$=76±3. For the calculation of EFs see Supplementary Tables 2,3 and Equation 1 (S29). Selections were performed in triplicate (see Supplementary Figure 21). **b**, Fluorescence polarization of FITC-labelled compounds **13** and **14** with CREBBP bromodomain and control bromodomains BRD4(1) and BPTF. Error bars indicate standard deviation of three measurements.

The asterisk (*) indicates the dissociation constant value (Kd). **c**, Snapshot of maxisorp plate carrying small-molecule ELISA of compounds **13** and **14** after addition of TMB and 1M H_2SO_4. The assay was performed in triplicate against immobilized CREBBP bromodomain. **d**, Chemical structures of selected compounds and building blocks.

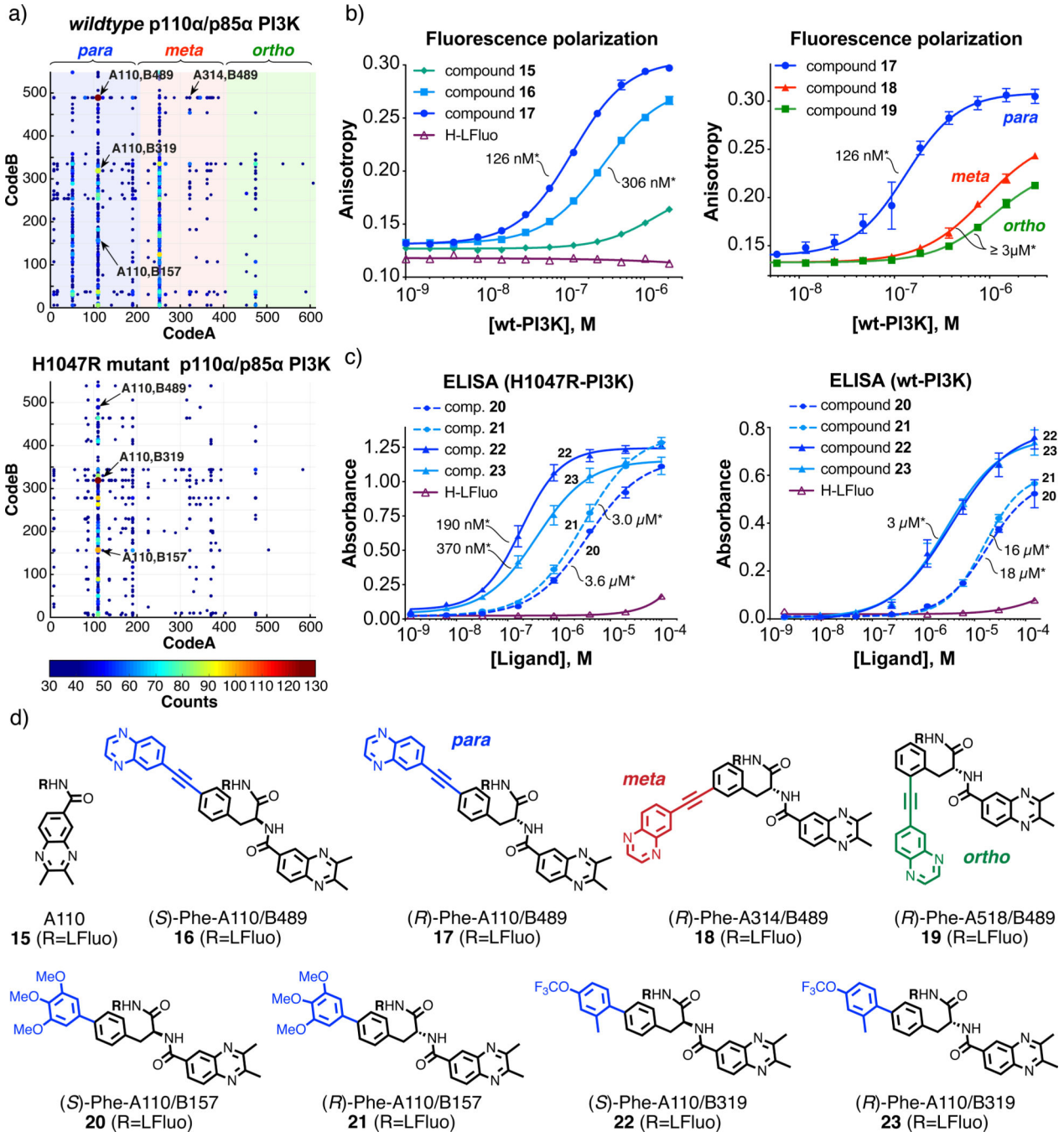

Figure 4 |. Selections against PI3KCA variants

a, Two-dimensional fingerprints of NF-DEL selections against the PI3Ks *wildtype* p110α/p85α PI3K (upper panel) and H1047R-p110α mutant of p110α/p85α PI3K (lower panel). The x and y axes represent the two building blocks while the color heat map shows the HTDS sequence counts. Building blocks A, corresponding to *para*- (1–204), *meta*- (205–408) and *ortho*- (409–612) regio-isomers, are highlighted in blue, red and green, respectively. Cut-off values equal to 25 (for *wt*-PI3K variant selection) and 30 (for H1047R mutant of PI3K variant selection) were applied to the fingerprints. The most

enriched building block combinations are indicated with arrows. For the calculation of EFs see Supplementary Tables 2,3 and **Equation 1** (S29). **b**, The binding of the most enriched combination (**A110/B489**, EF=65±7) against the *wildtype* protein corresponding to stereoisomers **15** and **16** was validated by fluorescence polarization and compared with a derivative of building block **A110** alone (**15**). The *meta*- and *ortho*-isomers of **17** corresponding to combinations **A314/B489** (**18**) and A518/B489 (**19**) were also measured for comparison. Error bars indicate standard deviation of three measurements. The asterisk (*) indicates the dissociation constant value (Kd). **c**, Enriched compounds corresponding to combinations **A110/B157** (**20** and **21**) and **A110/B319** (**22** and **23**) were validated by small-molecule ELISA against both H1047R mutant (left panel) and *wildtype* PI3K (right panel). Error bars indicate standard deviation of three measurements. The asterisk (*) indicates the dissociation constant value (Kd). **d**, Chemical structures of selected compounds.

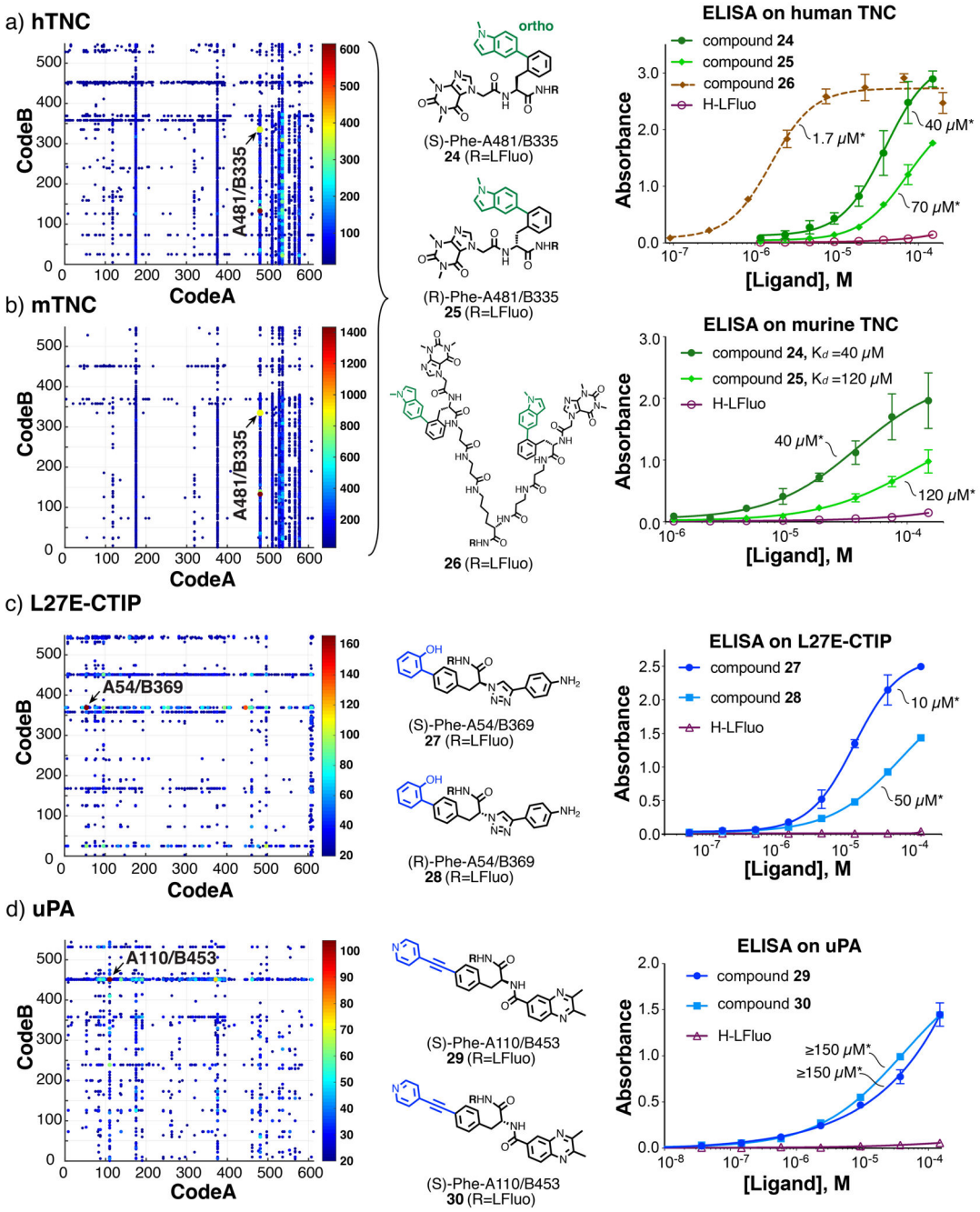

Figure 5 |. Selections against tumor-associated antigens and human CtIP.

Two-dimensional fingerprints of selections against: **a**, human tenascin-C (hTNC); **b**, murine tenascin-C (mTNC); **c**, the L27E mutant of N-terminal CtIP **d**, urokinase-type plasminogen activator (uPA). A cut-off value equal to 20 was applied to all the fingerprints. The most enriched combinations (**A481/B335** for hTNC and mTNC, **A110/B453** for uPA and **A54/B369** for L27E-CtIP) were re-synthesized off-DNA and validated by small-molecule ELISA. Error bars indicate standard deviation of three measurements. Details on DNA counts for individual library members, enrichment factors and dissociation constants are

reported in Supplementary Tables 2,3 and 6. The asterisk (*) indicates the dissociation constant value (Kd).